Eur. J. Biochem. 211, 37–45 (1993)

Flavin dynamics in reduced flavodoxins

A time-resolved polarized fluorescence study

Rik LEENDERS[1], Martin KOOIJMAN[1], Arie van HOEK[2], Cees VEEGER[1] and Antonie J. W. G. VISSER[1]

Departments of Biochemistry[1] and Molecular Physics[2], Agricultural University, Wageningen, The Netherlands

(Received May 25/September 11, 1992) – EJB 92 0729

The time-resolved fluorescence and fluorescence anisotropy characteristics of reduced flavin mononucleotide in solution as well as bound in flavodoxins isolated from the bacteria *Desulfovibrio gigas, Desulfovibrio vulgaris, Clostridium beijerinckii MP* and *Megasphaera elsdenii* have been examined. All fluorescence and fluorescence anisotropy decays were analyzed by two different methods: (a) least-squares fitting with a sum of exponentials and (b) the maximum entropy method to yield distributed lifetimes and correlation times. The results of both approaches are in excellent agreement. The fluorescence decay of the free as well as protein-bound reduced flavin chromophore is made up of three components. The shortest component proves to be relatively sensitive to the environment and can therefore be used as a diagnostic tool to probe the microenvironment of the reduced isoalloxazine ring system. The other two longer fluorescence lifetime components are insensitive to the chromophore environment and seem therefore to be related to intrinsic, photophysical properties of the reduced chromophore. Fluorescence anisotropy decays show that the flavin mononucleotide in all four reduced flavodoxins is immobilized within the protein matrix, as indicated by the recovery of a single rotational correlation time, reflecting the rotation of the whole protein. No indications are found that rapid structural fluctuations occur in reduced flavodoxins, and the mechanism of electron transfer from flavodoxin to other redox proteins seems to involve immobilized reduced flavin.

Flavodoxins are small (14–24-kDa) electron-transferring proteins which can be isolated from some algae and several anaerobic and aerobic bacteria grown under iron-deficient conditions [1, 2], although some bacteria also produce flavodoxin under iron-containing conditions [3–7]. Up to now, no flavodoxins have been found in higher animals or plants.

Flavodoxins promote electron transfer between two redox proteins as part of photosynthetic, nitrogen-reducing, sulfate-reducing or hydrogen-evolving systems (for a review see [8]). Based on biochemical and spectroscopic differences, flavodoxins can be divided into two groups: the *rubrum*-type and *pasteurianum*-type of flavodoxins [9].

Flavodoxins contain one non-covalently bound flavin mononucleotide (FMN) which can exist in three different oxidation states, i.e. oxidized, one-electron-reduced (semiquinone), and two-electron-reduced (hydroquinone). Under physiological conditions flavodoxins shuttle between the semiquinone and hydroquinone states and are thus one-electron-transferring proteins.

Chemical composition and amino acid sequence are known for quite a number of flavodoxins, while for a few flavodoxins in the oxidized state three-dimensional structures have been elucidated [10–13]. Furthermore, the structures of semiquinone and reduced *Clostridium beijerinckii* flavodoxin [14, 15], semiquinone and reduced *Desulfovibrio vulgaris* flavodoxin [16] and reduced *Megasphaera elsdenii* flavodoxin [17] have been published. The overall structures of these flavodoxins in their different oxidation states are highly similar, except for some variations in protein conformation and amino acid composition around the flavin chromophore. It has been shown that in reduced *Cl. beijerinckii* flavodoxin the protein backbone of residue Gly57 is rotated towards the flavin, facilitating hydrogen bonding between the apoprotein and the flavin molecule [14]. Recently, Watt et al. [16] demonstrated a similar conformational change for reduced *D. vulgaris* flavodoxin. Nuclear magnetic resonance studies of *D. vulgaris* flavodoxin have revealed a hydrogen bond between the flavin atom N(1) and residue Asp95 in all three oxidation states [18], implying that atom N(1) remains unprotonated upon reduction. These studies confirmed a similar finding in the three different oxidation states of *Cl. beijerinckii* flavodoxin [14].

Comparison of the structures of oxidized *D. vulgaris* and *Cl. beijerinckii* flavodoxin [8] shows a high degree of similarity between the folding of the polypeptide chains, but differences in the flavin binding sites exist. Firstly, the orientation of the isoalloxazine rings with respect to the otherwise aligned crystallographic protein structures are at 24° to each other. Secondly, the distance between the flavin N(5) and the carbonyl oxygen of the rotated glycine residue is somewhat shorter in *Cl. beijerinckii* flavodoxin (0.28 nm) as compared to *D. vulgaris* flavodoxin (0.30 nm). Furthermore, the tryptophan residue which is located near the active site in *D. vulgaris* flavodoxin is not stacked with the isoalloxazine of the flavin (the tryptophan–flavin center-to-center distance is 0.55 nm), whereas in *Cl. beijerinckii* flavodoxin residue Trp90 seems

Correspondence to A. J. W. G. Visser, Department of Biochemistry, Agricultural University, Dreijenlaan 3, NL-6703 HA Wageningen, The Netherlands

to be stacked with the flavin chromophore (center-to-center distance is 0.31 nm). Based on nearly identical tryptophan fluorescence results, it was noted that *Desulfovibrio gigas* and *D. vulgaris* flavodoxins have a very similar tryptophan residue in common [19]. Although only limited information about proton – proton distances between the flavin molecule and the *M. elsdenii* apoflavodoxin is available from two-dimensional ^{1}H-NMR studies [13, 17], it seems that in this flavodoxin the flavin is stacked with a tryptophan residue (Trp91).

These differences in flavin environment are reflected in the spectroscopic properties of the flavodoxins. Shifted absorption maxima and different ellipticity cross-over points in visible circular dichroic spectra between both classes of flavodoxins result in two clearly distinguishable flavodoxin types [9]. Redox properties [8] and Raman spectroscopy also revealed significant differences in flavin vibrational frequencies in bacterial flavodoxins belonging to the two classes [20].

There is cumulating evidence for the existence of rapid structural fluctuations in proteins and attention is being focussed to relate these fluctuations with biochemical reactions [21 – 23]. Such fluctuations may play an important role in the mechanism of electron transfer of flavodoxins.

Since crystallographically obtained structures contain only limited information about internal dynamics, other spectroscopic techniques have to be applied to obtain more detailed information. Time-resolved protein fluorescence is widely used to investigate structure and dynamics (for general references see [24 – 28]). Both segmental motion of a chromophore and isotropic rotation of a whole protein can be observed using high-resolution fluorescence techniques. The most intensively studied probe is tryptophan but other intrinsic probes, like tyrosine and flavin, and extrinsic probes can also be used to study protein dynamics. We have employed sensitive time-resolved fluorescence and fluorescence anisotropy techniques to obtain information on the dynamic characteristics of reduced flavin in flavodoxins. Reduced flavins are intrinsically fluorescent and their fluorescence properties have been globally investigated for several reduced model compounds and flavoproteins [29 – 31]. The fluorescence of reduced (1,5-dihydro) flavins, free or bound in flavodoxin as dealt with in this article, has in general a rather low quantum yield, which is in contrast to the fluorescence quantum yield of 4a,5-dihydroflavins [32]. Four reduced flavodoxins were investigated: *D. gigas* and *D. vulgaris* flavodoxin as members of the *rubrum* class of flavodoxins and *Cl. beijerinckii* and *M. elsdenii* flavodoxin as members of the *pastaurianum* class of flavodoxins. The results are compared with the dynamic fluorescence properties of free reduced flavin mononucleotide.

MATERIALS AND METHODS

Preparation of the flavodoxins

The preparation of flavodoxins from *D. gigas, D. vulgaris, Cl. beijerinckii*, and *M. elsdenii* was as described previously [2, 7, 33, 34]. Flavin mononucleotide (FMN) was obtained from Merck. FMN and the flavodoxins were dissolved in 70 mM sodium diphosphate pH 8.3 at concentrations which varied over 50 – 150 μM. These concentrations, rather high for optical spectroscopy, were necessary because of the low absorbance of the reduced chromophore at the excitation wavelength. The anaerobic solutions were reduced by the addition of equimolar amounts of sodium dithionite as described by Ghisla et al. [29]. Substoichiometric amounts of dithionite would result in incomplete reduction and remaining small traces of oxidized flavodoxin would cause a disturbing signal because of its significantly higher quantum yield of fluorescence. All chemicals used were of the highest purity available and only Millipore-filtered water was used. All experiments were conducted between 4 – 37 °C.

Time-resolved fluorescence and fluorescence anisotropy measurements

Fluorescence and fluorescence anisotropy decays were measured using the time-correlated single-photon-counting technique [35 – 40]. Reduced free and protein-bound flavin was excited at 444.0 nm with vertically polarized light. Erythrosin B served as a reference compound to yield the instrumental response function (erythrosin B shows a single exponential fluorescence decay with a slightly temperature-dependent lifetime, which amounts to 80 ps at 20 °C). After excitation the parallel and perpendicular polarized fluorescence intensities were monitored using a 557.9-nm line filter (Schott with half-band width of 13.0 nm) in combination with a cut-off filter (Schott OG530). In this way the disturbing Raman scattering signal of water is not detected and only fluorescence photons are detected and accumulated in discrete channels of the multichannel analyzer. Due to the relatively low fluorescence quantum yields of the reduced flavodoxins, the background fluorescence arising from the buffer had to be subtracted, since it amounted to a small percentage of the protein fluorescence. The fluorescence and fluorescence anisotropy decays were analyzed by two different methods. The total fluorescence decays were analyzed by nonlinear least-squares fitting of the experimental data with a sum of exponentials [40]:

$$f(t) = i_{\parallel}(t) + 2g i_{\perp}(t) = \sum_{i=1}^{n} \alpha_i e^{-t/\tau_i} \quad \text{with } i = 1, 2, \ldots n \qquad (1)$$

where $f(t)$ is the deconvoluted time-dependent fluorescence, $i_{\parallel}(t)$ and $i_{\perp}(t)$ are the parallel and perpendicular polarized fluorescence components, and g is the correction factor for the different responses of the instrumentation to parallel and perpendicular polarized light. Polarizers were aligned carefully and, when measuring reference samples of known anisotropy, it was found that no correction was needed (g-factor is 1). α_i and τ_i are the relative contribution and fluorescence lifetime of component i, respectively. The fluorescence anisotropy decays, $r(t)$, were globally analyzed in an analogous manner:

$$r(t) = \sum_{j=1}^{m} \beta_j e^{-t/\phi j} \quad \text{with } j = 1, 2, \ldots m \qquad (2)$$

where m is the number of rotational correlation time components, β_j and ϕ_j are the amplitude and rotational correlation time of component j, respectively. The sum of β_j corresponds to the initial anisotropy r_0. The parallel and perpendicular fluorescence decays were globally analyzed by minimizing the reduced χ^2 statistics:

$$\chi^2 = \frac{1}{N} \sum_{k=1}^{N} \frac{\{I_k^{\text{calc}} - I_k^{\text{obs}}\}^2}{\sigma_k^2} \qquad (3)$$

where N is the number of degrees of freedom, I_k^{calc} and I_k^{obs} are the calculated and observed number of photons in channel k, respectively. Furthermore, σ_k^2 is the variance in channel k.

The fluorescence decay as well as the fluorescence anisotropy decay were also analyzed in terms of a continuous

distribution of decay times by means of the maximum entropy method (developed and distributed by Maximum Entropy Data Consultancy Ltd, Cambridge, UK). In this method [41, 42], a spectrum of decay times, $\alpha(\tau)$, can be recovered by considering the total fluorescence, $I(t)$:

$$I(t) = I_{\parallel}(t) + 2gI_{\perp}(t) = E(t) * \int_0^{\infty} \alpha(\tau)\, e^{-t/\tau}\, d\tau \qquad (4)$$

where $I(t)$ is the sum of the polarized fluorescence intensities [$I_{\parallel}(t)$ and $I_{\perp}(t)$] which are convolved (represented by the symbol *) with the shape of the excitation pulse, $E(t)$. $\alpha(\tau)$ represents the number of fluorophores that decay with time constant τ. The image $\alpha(\tau)$, which is formally the inverse Laplace transform of the measured intensities deconvolved from the excitation pulse $E(t)$, is calculated in such a way that it results in a maximum value of the Skilling-Jaynes entropy, S [43]:

$$S = \int_0^{\infty} \alpha(\tau) - m(\tau) - \alpha(\tau) \log \frac{\alpha(\tau)}{m(\tau)}\, d\tau \qquad (5)$$

where $m(\tau)$ is the starting model for the distribution of fluorescence lifetimes. The entropy is maximized under the condition that the reduced χ^2 (Eqn 3) is minimized [43]. When no *a priori* knowledge about the shape of the distribution was available, $m(\tau)$ was set to a flat distribution in $\log(\tau)$ space as this introduces the least correlations between the $\alpha(\tau)$ parameters [42, 44].

From fluorescence anisotropy experiments one can recover the complete three-dimensional image $\gamma(\tau,\phi,r_0)$, representing the number of fluorophores with lifetime τ, rotational correlation time ϕ, and initial anisotropy r_0 [42]. If one assumes that τ and ϕ are uncorrelated (non-associative model) the images $\alpha(\tau)$ and $\beta(\phi)$ are independent as expressed by the deconvolved polarized fluorescence intensity components:

$$i_{\parallel}(t) = \frac{1}{3} \int_0^{\infty} \alpha(\tau)\, e^{-t/\tau}\, d\tau \int_0^{\infty} \{1 + 2\beta(\phi)\}\, e^{-t/\phi}\, d\phi \qquad (6)$$

and

$$i_{\perp}(t) = \frac{1}{3} \int_0^{\infty} \alpha(\tau)\, e^{-t/\tau}\, d\tau \int_0^{\infty} \{1 - \beta(\phi)\}\, e^{-t/\phi}\, d\phi \qquad (7)$$

where the integrated amplitude $\beta(\phi)$ corresponds to the initial anisotropy r_0, which is dependent on the degree of non-coincidence of absorption and emission transition moments, and r_0 may be defined by an (average) angle ζ between them:

$$r_0 = 1/5\,(3\cos^2\zeta - 1). \qquad (8)$$

A spectrum of rotational correlation times ϕ, $\beta(\phi)$, is obtained for which it also applies that, if no *a priori* knowledge of the distribution is known, the initial spectrum should be taken flat in $\log(\phi)$ space.

In the analysis of the fluorescence decay an $\alpha(\tau)$ image consisting of 150 decay times equally spaced in $\log(\tau)$ space (ranging over 0.01 – 15 ns) was recovered. This image was then fixed in the anisotropy decay analysis where an image $\beta(\phi)$ consisting of 150 rotational correlation times equally spaced in $\log(\phi)$ space (0.05 – 30 ns) was recovered.

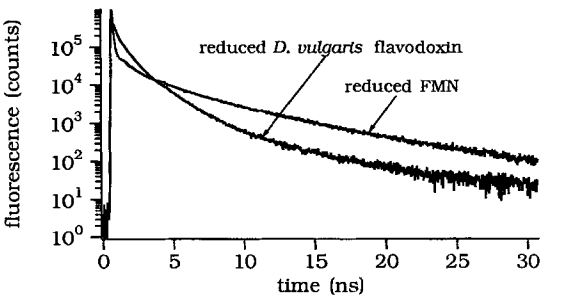

Fig. 1. Fluorescence decay curves of reduced *D. vulgaris* flavodoxin and reduced free FMN. Both fluorescence decays were measured at 4 °C. Excitation and emission wavelengths were 444.0 nm and 557.9 nm, respectively (see text for details).

RESULTS AND DISCUSSION

Time-resolved fluorescence

As an example, the time-resolved fluorescence intensity of reduced *D. vulgaris* flavodoxin at 4 °C is presented in Fig. 1. The fluorescence intensity of reduced free FMN, which is also given for comparison, initially decays much faster than the fluorescence intensity of the reduced protein. It is obvious from the semilogarithmic display in Fig. 1 that the time-dependent fluorescence intensities exhibit a heterogeneous pattern. When the fluorescence decays of reduced free FMN and the reduced flavodoxins were analyzed by non-linear least-squares fitting procedures using a sum of exponentials (Eqn 1), at least three exponentials were needed to describe the experimental decay adequately. The fitting parameters obtained are listed in Table 1. It is to be noted that the relative contributions of the different fluorescence lifetime components are more or less independent of the flavodoxin species. In general, 80% of the total fluorescence decay is that of the shortest fluorescence lifetime component, τ_1, and lifetime components τ_2 and τ_3 are present with relative contributions of 19% and 1%, respectively. The shortest fluorescence lifetime in free reduced FMN is shorter than in reduced flavodoxins, where it seems to be class-dependent. Flavodoxins from the *rubrum* class (the two *Desulfovibrio* flavodoxins) have a significantly shorter τ_1 (about 400 ps) than flavodoxins from the *pasteurianum* class (τ_1 of about 750 ps). The values of τ_2 and τ_3 seem to be independent of the kind of flavodoxin and, hence, of the environment of the reduced flavin chromophore.

The fluorescence decay curves of all four reduced flavodoxins as well as free reduced flavin were analyzed using the maximum entropy method, in order to obtain information about the distribution of lifetimes in the decays. The results of these analyses are shown in Fig. 2. From inspection of Fig. 2, it is clear that indeed more than one component is present in the decays. A common feature in the distributions of reduced free and protein-bound flavin is the presence of three lifetime distributions in accordance with the results obtained with the least-squares fitting. The fluorescence decay of free reduced flavin is composed of a most intense distribution peaked at about 115 ps, and two other distributions with barycenters at about 1.3 ns and 4.5 ns (see Table 1). The relative contributions of these components are 82%, 17% and 1%, respectively. In the *Desulfovibrio* flavodoxins an intense distribution (about 77% of the total fluorescence) of a shorter lifetime component is found at about 350 ps, and two other less intense distributions at about 1.3 ns and 3 – 4 ns (about

Table 1. Fluorescence decay characteristics of reduced FMN and reduced flavodoxins (at 4°C). Parameters were obtained by least-squares fitting of the time-resolved fluorescence (Eqn 1). Excitation and emission wavelengths were 444.0 nm and 557.9 nm, respectively. The order of magnitude of the errors (given in parenthesis) is deduced from the results of multiple experiments. The average fluorescence lifetime is defined as: $\langle\tau\rangle = \Sigma\alpha_i\tau_i$ (Eqn 12). χ^2 is defined by Eqn (3). Q was calculated according to Eqn (9) using $\tau_0 = 56$ ns (see text).

Sample	α_1 (±0.02)	τ_1 (±0.02)	α_2 (±0.02)	τ_2 (±0.15)	α_3 (±0.02)	τ_3 (±0.25)	$\langle\tau\rangle$	χ^2	Q
		ns		ns		ns			
FMN	0.80	0.12	0.19	1.41	0.01	5.27	0.30	1.02	0.005
D. gigas	0.80	0.44	0.19	1.71	0.01	4.40	0.72	1.16	0.013
D. vulgaris	**0.79**	**0.39**	**0.19**	**1.41**	**0.02**	**4.11**	**0.66**	**1.13**	**0.012**
Cl. beijerinckii	0.75	0.88	0.23	1.30	0.02	4.53	1.05	1.09	0.019
M. elsdenii	0.82	0.72	0.15	1.47	0.03	5.26	0.97	1.02	0.017

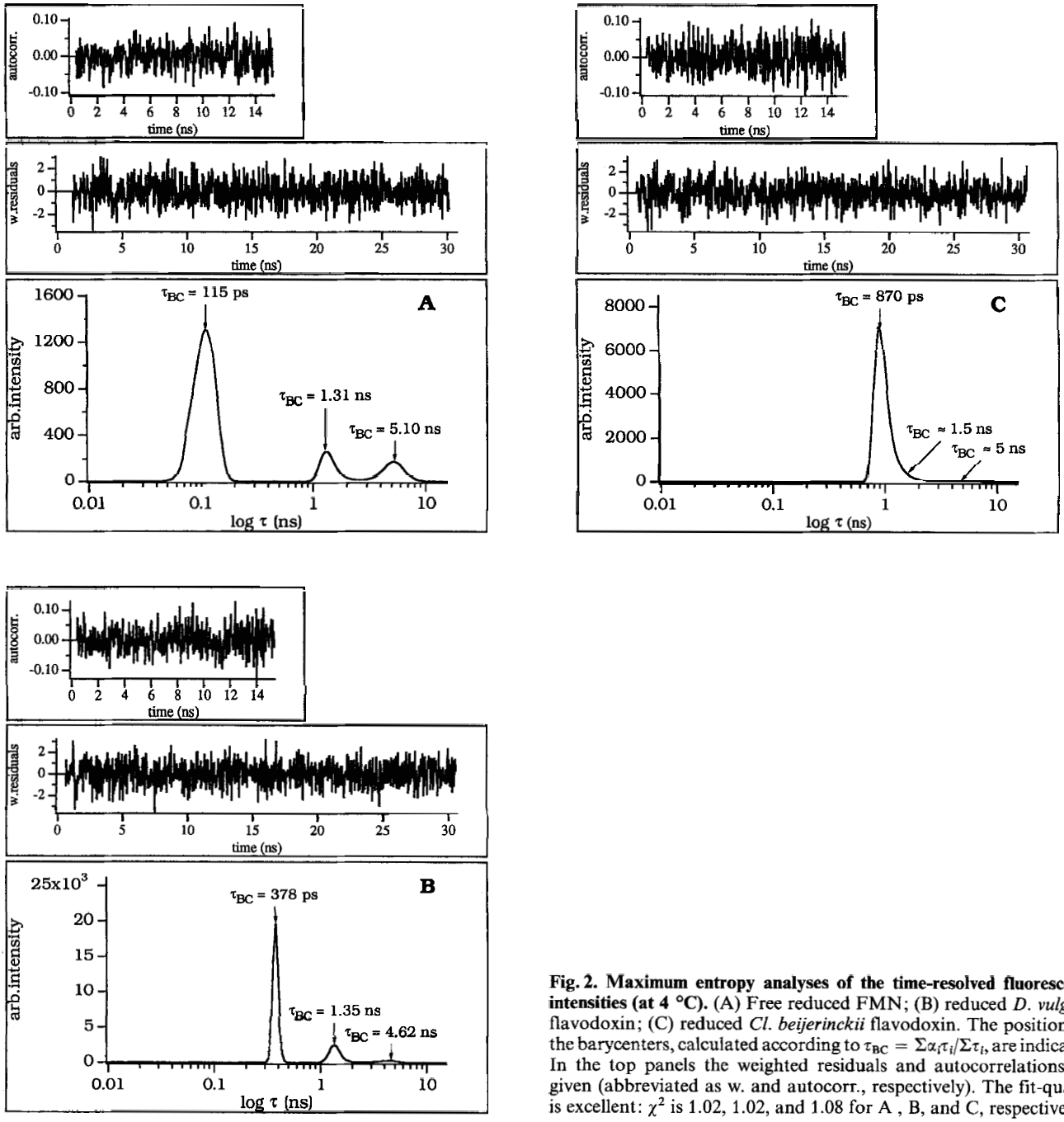

Fig. 2. Maximum entropy analyses of the time-resolved fluorescence intensities (at 4 °C). (A) Free reduced FMN; (B) reduced *D. vulgaris* flavodoxin; (C) reduced *Cl. beijerinckii* flavodoxin. The positions of the barycenters, calculated according to $\tau_{BC} = \Sigma\alpha_i\tau_i/\Sigma\tau_i$, are indicated. In the top panels the weighted residuals and autocorrelations are given (abbreviated as w. and autocorr., respectively). The fit-quality is excellent: χ^2 is 1.02, 1.02, and 1.08 for A , B, and C, respectively.

20% and 3% of the total fluorescence, respectively). In *Cl. beijerinckii* and *M. elsdenii* flavodoxin an intense lifetime distribution is found at about 800 ps, i.e. considerably longer than the corresponding short lifetimes in *Desulfovibrio* flavodoxins. The asymmetric form of this distribution (see Fig. 2C) indicates an underlying lifetime component at about 1.5 ns. A third lifetime distribution is present which could not be very well resolved.

Fluorescence techniques with high time resolution show that the fluorescence decays of reduced flavodoxins are not monoexponential, in contrast to earlier findings in which the decay of reduced *M. elsdenii* flavodoxin appeared to be consistent with a single fluorescence lifetime of 2.1 ns [30]. The existence of three fluorescence lifetime components is now demonstrated. It is difficult to explain the exact origin of this fluorescence lifetime heterogeneity, but the observation that the fluorescence is enhanced in more rigid structures [30] indicates that the shortest fluorescence lifetime (τ_1) is influenced by the environment of the flavin. It is noted that, because of the smaller distance between the flavin and the rotated glycine carbonyl oxygen, the reduced flavin in *Cl. beijerinckii* flavodoxin is probably bound more firmly than in *D. vulgaris* flavodoxin. The longer lifetimes (τ_2 and τ_3) possibly originate from flavin configurations which are almost or completely planar (*vide infra*). Comparison of the fluorescence decays of free and protein-bound reduced FMN indicates that no additional exponential components are introduced as a result of changes in micro-environment of the isoalloxazine ring system.

The results show that the position of the shortest lifetime distribution is influenced by the environment of the flavin chromophore. In free reduced FMN τ_1 is about 115 ps and in reduced flavodoxins τ_1 is significantly longer (about 400 ps in *rubrum* flavodoxins and about 800 ps in *pasteurianum* flavodoxins). Two possible mechanisms both explaining this behaviour can be proposed. The reduced chromophore in solution is completely surrounded by water molecules. The excited state will therefore be immediately stabilized to a solvent-relaxed state which might be deactivated more efficiently by radiationless transition to the ground state (internal conversion) than is the unrelaxed excited state. This would mainly be reflected by a considerable shortening of the average lifetime of the excited state. An alternative and/or additional mechanism has been proposed which may also account for the multiplicity of decay times observed [31]. Ultrafast (subpicosecond) collective vibrations are responsible for the fact that reduced flavin possesses multiple conformations of different planarity. Upon excitation most nonplanar states will return to the ground state via radiationless pathways which explains the picosecond lifetimes observed in most reduced flavin compounds in fluid solutions. In reduced flavodoxins the isoalloxazine ring system is (partially) surrounded by a more rigid protein environment resulting in a decreased rate of internal conversion and an increased τ_1. The so-called butterfly motion, i.e. inversion of the central ring as detected in reduced flavins in solution [45], will be hindered by the protein environment and may be expected to reduce the rate of radiationless transitions to the ground state (the energy dissipates better in more dynamic systems). As a result of the partial accessibility of the reduced protein-bound flavin, solvent relaxation will play a less important role as compared to reduced flavins in solution leading to longer lifetimes.

The value of τ_1 can be used as a diagnostic tool for probing the environment of reduced flavin chromophores. This influence is smaller in the *rubrum* class than in the *pasteurianum*

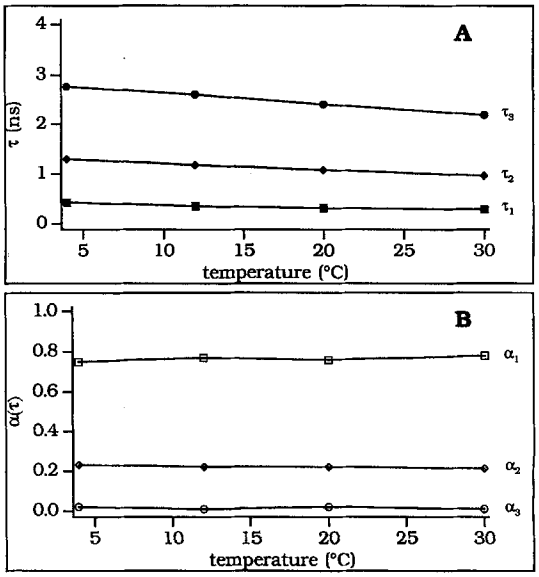

Fig. 3. Position of the barycenters, τ_i, and integrated amplitudes, α_i, of the separate fluorescence lifetimes in reduced *D. gigas* flavodoxin as a function of temperature. (A) Position of the barycenters; (B) integrated relative amplitudes.

class of flavodoxins: the flavin in the former proteins has dynamic properties which are more similar to reduced flavin in solution. The flavin in the latter class of flavodoxins is more restricted by the protein environment, probably as a result of a more intense hydrogen bonding between the flavin N(5) and H(5) atoms and the rotated glycine carbonyl oxygen.

An interesting feature is detected at increased temperatures and occurs in all four reduced flavodoxins, as well as in reduced FMN in solution. All fluorescence lifetimes shorten at higher temperature, but they do not converge, whereas their relative contributions (α_i) are clearly independent of temperature. This is illustrated in Fig. 3 for reduced *D. gigas* flavodoxin. This appears to rule out excited-state processes such as exciplex formation or solvent relaxation on the time scale of the emission itself, because the resultant lifetime changes would also affect the α terms. The fact that the α values do not vary with temperature favours the excited-state kinetics in which there are three independently emitting species. These emitting conformers either result from three different ground states or are formed in parallel very rapidly (non-exchangeable) in the excited state by a temperature-independent mechanism both in free solution and when bound in flavodoxin. The lack of interconversion between the separate emitting forms indicates that the energy barrier between configurations is too high and therefore no major conformational changes occur [46]. Reduced flavodoxins were measured up to 37 °C and showed no sign of degradation, whereas fluorescence of reduced FMN in solution (above 20 °C) decreased to a non-detectable level.

The fluorescence quantum yield, Q, of an aromatic molecule exhibiting a monoexponential excited-state decay is related to its measured lifetime τ by:

$$Q = \frac{\tau}{\tau_0} \tag{9}$$

where τ_0 is the 'natural' fluorescence lifetime, i.e. that which would be observed in the absence of radiationless deactivation of the excited singlet state. This latter lifetime, also called the

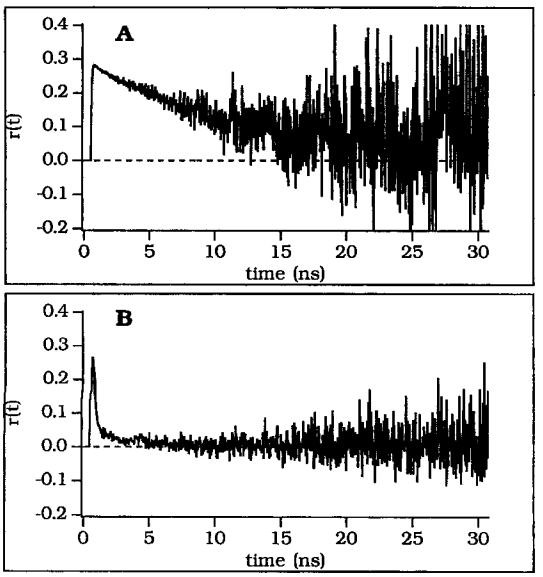

Fig. 4. Fluorescence anisotropy decays of reduced flavin in solution and in flavodoxin (at 4 °C). (A) Reduced *D. vulgaris* flavodoxin; (B) reduced FMN in solution. The anisotropy of free reduced flavin decays much faster than that of reduced flavodoxin (see Table 2).

radiative lifetime, can be estimated from the first absorption and emission bands according to [47]:

$$\frac{1}{\tau_0} = 2.88 \times 10^{-9} n^2 \langle \tilde{\nu}_F^{-3} \rangle^{-1} \int_0^\infty \frac{\varepsilon(\tilde{\nu})}{\tilde{\nu}} \mathrm{d}\tilde{\nu} \qquad (10)$$

where n is the refractive index of the medium, ε the absorption coefficient (in M^{-1} cm^{-1}) and $\tilde{\nu}$ the wavenumber (cm^{-1}). $\langle \tilde{\nu}_F^{-3} \rangle$ is the third moment of the fluorescence spectrum defined as:

$$\langle \tilde{\nu}_F^{-3} \rangle = \frac{\int_0^\infty \tilde{\nu}^{-3} F(\tilde{\nu}) \mathrm{d}\tilde{\nu}}{\int_0^\infty F(\tilde{\nu}) \mathrm{d}\tilde{\nu}}. \qquad (11)$$

Using Eqns (10) and (11) it was calculated for reduced *Cl. beijerinckii* flavodoxin that τ_0 is 56 ns. Assuming that τ_0 is invariant to the environment of the chromophore, any variation in quantum yield can be attributed to differing magnitudes of the rate constants for radiationless deactivation. For multi-exponential fluorescence decay the value for τ can be taken as the average fluorescence lifetime, $\langle \tau \rangle$ (according to [48]):

$$\langle \tau \rangle = \sum_{i=1}^{n} \alpha_i \tau_i \quad (\text{with} \sum_{i=1}^{n} \alpha_i = 1) \qquad (12)$$

provided that each component arises from an independent monoexponentially decaying excited-state species with identical radiative lifetime and spectral distribution for each of the individual forms. The average excited-state lifetime of reduced FMN in solution ($\langle \tau \rangle$ is 0.30 ns) is significantly smaller than for protein-bound reduced FMN ($\langle \tau \rangle$ varies between 0.66–1.05 ns for the different flavodoxins). This means that the quantum yield, calculated by substitution of $\langle \tau \rangle$ and τ_0 in Eqn (9), increases upon binding of the reduced chromophore (Table 1), which is in agreement with steady-state fluorescence intensity measurements (data not shown). Therefore, for reduced flavodoxins the rate of radiationless deactivation of the excited state is smaller than for free reduced FMN.

Table 2. Fluorescence anisotropy decay characteristics of reduced free FMN and reduced flavodoxins (at 4°C). The parameters were obtained by least-squares fitting of the time-resolved fluorescence anisotropy (Eqn 2, $j = 1$). The order of magnitude of the errors (in parenthesis) is based on results obtained from multiple experiments.

Sample	β (±0.01)	ϕ (±0.14)	χ^2
		ns	
FMN	0.30[a]	0.22	1.14
D. gigas	0.29	11.96	1.01
D. vulgaris	0.28	11.18	1.16
Cl. beijerinckii	0.25	9.73	1.08
M. elsdenii	0.25	9.13	1.13

[a] This value was fixed.

Time-resolved fluorescence depolarization

We also performed time-resolved fluorescence depolarization experiments on members of the two classes of flavodoxins to investigate whether differences in flavin microenvironments are related to an altered motional behaviour. In Fig. 4 it is demonstrated that the fluorescence anisotropy decay of free reduced FMN (at 4°C) is significantly faster than that of reduced *Cl. beijerinckii* flavodoxin. When the fluorescence anisotropy decay is analyzed using a sum of exponentials it is found that a single exponential is sufficient yielding a rotational correlation time of 220 ps for free reduced flavin at 4°C (Table 2). This value is somewhat smaller than the rotational correlation time found for oxidized flavin mononucleotide at the same temperature [49] (and Leenders et al., unpublished results), which is possibly due to a reduced hydration sphere around the molecule. The fluorescence anisotropy decay of reduced flavodoxins could also be described with a single exponential (an additional anisotropy component did not result in better fits). The rotational correlation times of reduced flavodoxins as obtained with least-squares fitting are listed in Table 2.

The fluorescence anisotropy decays of the four reduced flavodoxins and free reduced flavin were also analyzed using the maximum entropy method. The results of these analyses at 20°C are shown in Fig. 5. It is clear that the anisotropy of all reduced flavodoxins can be described by a unimodal distribution of correlation times. Using the empirical formula [50] describing the relation between the molecular mass of a protein and the rotational correlation time ϕ (in ns) at room temperature, (20°C):

$$\phi = 3.84 \times 10^{-4} M_r \qquad (13)$$

where M_r is the relative molecular mass, a spherical protein like flavodoxin, with an M_r of 15000, would have a rotational correlation time of about 5.8 ns at 20°C. In all four reduced flavodoxins the barycenters of the distribution of correlation times are of this order (Fig. 5), indicating that the reduced flavin is immobilized within the protein matrix, and hence rotates with the whole protein. In the *pasteurianum* class of

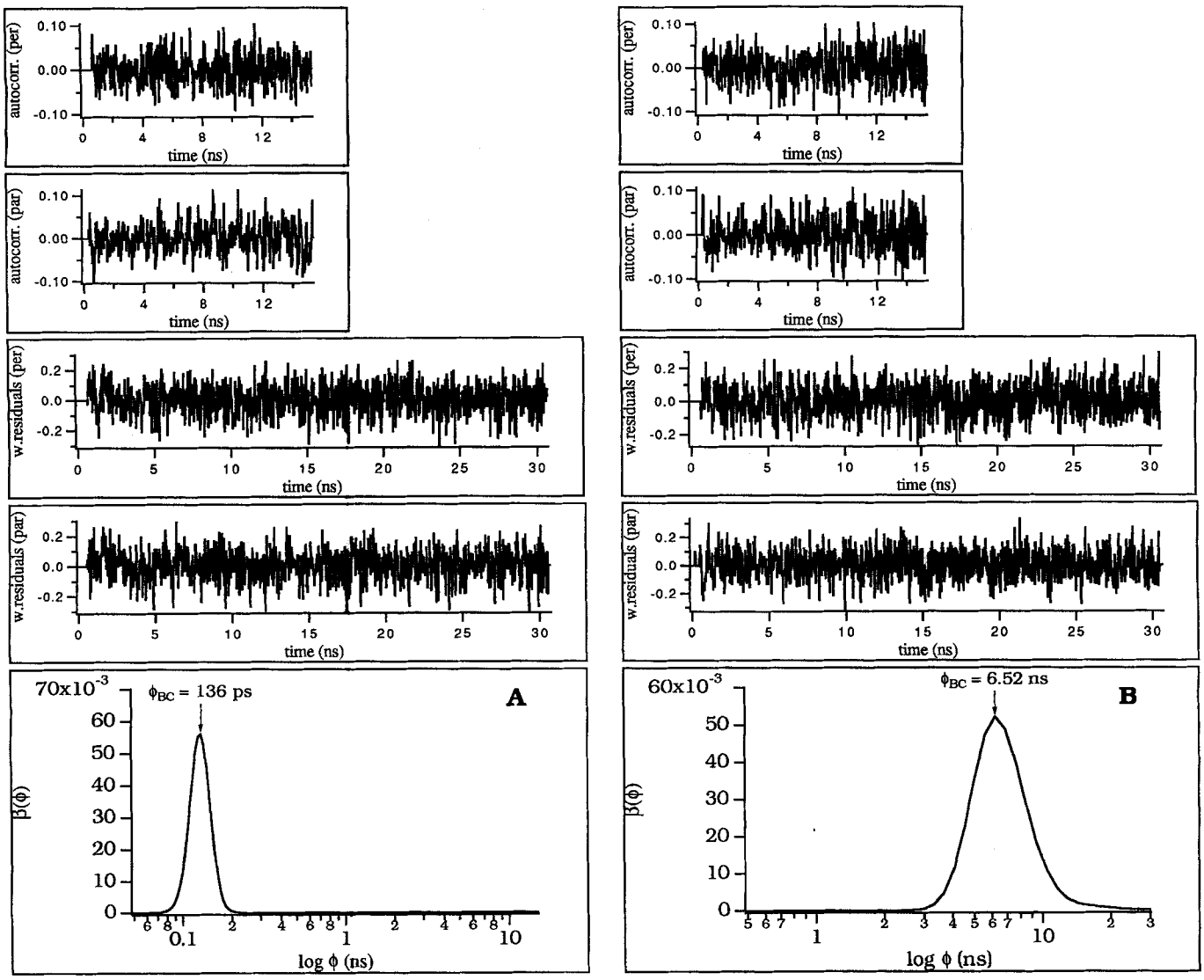

Fig. 5. Maximum entropy analyses of the time-resolved fluorescence anisotropies (at 20 °C). (A) Reduced FMN in solution; (B) reduced *D. vulgaris* flavodoxin; (C) reduced *Cl. beijerinckii* flavodoxin. The positions of the barycenters, calculated according to $\phi_{BC} = \Sigma\beta_i\phi_i/\Sigma\phi_i$, are indicated. Integration of the amplitudes $\beta(\phi)$ yields different initial anisotropies for reduced *Cl. beijerinckii* and *D. vulgaris* flavodoxins of 0.249 ± 0.002 and 0.281 ± 0.003, respectively (the errors are standard deviations deduced from integration of five separate measurements). In the top panels the weighted residuals and autocorrelations for the parallel and perpendicular components are given (abbreviated as w., autocorr., par., and per., respectively). The fit-quality of the presented analyses is excellent: χ^2 is 1.09, 1.05, and 1.06 for A , B, and C, respectively.

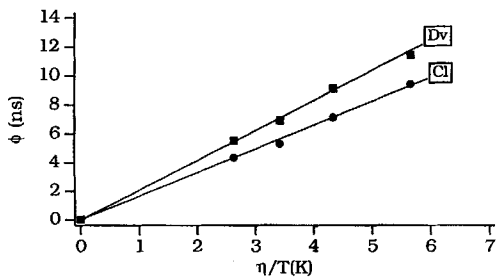

Fig. 6. Relative viscosity dependence of the rotational correlation times of reduced *D. vulgaris* (Dv) and *Cl. beijerinckii* (Cl) flavodoxin as obtained from the barycenters of the correlation time distribution. A linear fit to the data is also given (with correlation coefficients of 0.99). The linear behaviour is consistent with the Stokes-Einstein relation (Eqn 14).

flavodoxins, a distribution of rotational correlation times is found which seems somewhat smaller than found in the *rubrum* class of flavodoxins. It is known that members of the *rubrum* class of flavodoxins contain about 10 extra amino acids and therefore the enlarged molecular mass will be reflected in the rotational correlation times. Analysis of temperature-dependent anisotropy decays using the maximum entropy method show that the rotational correlation times of both classes of flavodoxins (Fig. 6) shorten at higher temperature consistent with the Stokes-Einstein relation:

$$\phi = \frac{\eta V}{kT} \tag{14}$$

where ϕ is the rotational correlation time, η is the relative viscosity, V is the volume of the spherical rotating unit, k is the Boltzmann constant (1.38×10^{-23} J K^{-1}) and T is the

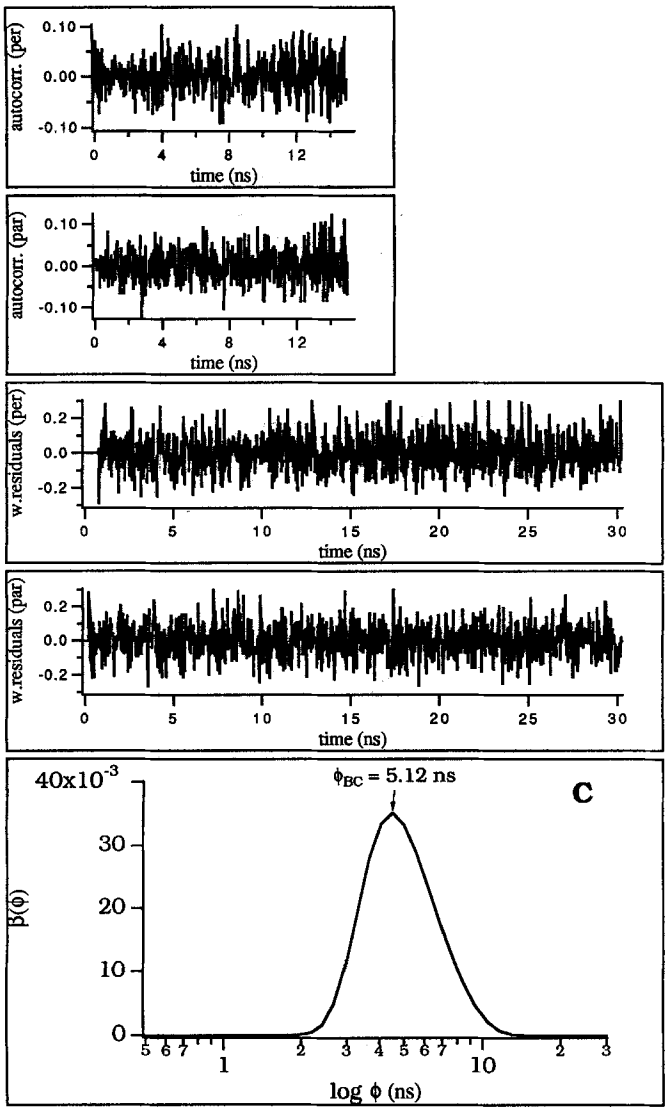

Fig. 5.

temperature in kelvin. No indications were found that the reduced protein-bound flavin chromophore exhibits any internal flexibility at elevated temperatures (37 °C).

It should be noted that long fluorescence lifetime components are the carrier signals for the anisotropy. Since the average fluorescence lifetime of reduced flavodoxins is about tenfold smaller than the rotational correlation times, the accuracy of the correlation times will be diminished, resulting in broader distributions of the rotational correlation times as compared to free reduced FMN.

From crystallographic and two-dimensional NMR studies [10–17] it is known that in flavodoxins aromatic amino acid residues are located within a small distance from the isoalloxazine ring of FMN. Furthermore, these studies indicated that upon reduction of the flavodoxins a polypeptide carbonyl group is rotated towards the reduced flavin and the reduced flavin becomes hydrogen-bonded with the apoprotein. Therefore, the reduced isoalloxazine ring system is buried in the flavin-binding site, resulting in immobilization of the flavin chromophore, consistent with the single correlation time found for whole protein rotation.

Integration of the amplitudes $\beta(\phi)$ yields significantly different initial anisotropies for reduced *pasteurianum* and *rubrum* flavodoxins of 0.249 ± 0.002 and 0.281 ± 0.003, respectively (see Fig. 5). These values are in excellent agreement with those obtained using least-squares fitting (Table 2). The reason that the initial anisotropies (r_0) are smaller than the theoretical maximum of 0.4, is certainly due to non-coincidence of absorption and emission transition moments. An average angle ξ between these moments can be calculated from the initial anisotropies using Eqn (8). For the *rubrum* and *pasteurianum* class of reduced flavodoxins these angles are $26.4 \pm 0.2°$ and $30.1 \pm 0.3°$, respectively, which is significantly larger than the angle found in oxidized flavodoxins (Leenders et al., unpublished results). These larger angles might be due to either overlapping of different electronic transitions or to differences in torsional vibrations [51] in oxidized and reduced isoalloxazine systems. It is noted that fluorescence studies using oriented flavodoxin crystals would have to be performed to determine the exact (mean) location of the absorption and emission dipole moment in reduced flavin [52].

The results described above may indicate that the rigidity of the reduced flavin chromophore observed and the spatial orientation that this implies is necessary for efficient oxidation of the reduced protein-bound flavin, after the flavodoxin is associated with other redox proteins [53]. Further studies investigating flavin dynamics in multi-redox complexes will contribute to the elucidation of the electron transfer mechanism.

Conclusions

The fluorescence intensity decay of reduced free FMN differed from that of reduced protein-bound FMN. However, similar peaks in the fluorescence lifetime distributions found in free reduced FMN were recovered in the reduced protein-bound flavins. Comparison of the fluorescence lifetimes/lifetime distributions showed that the lifetime of the shortest component is influenced by the protein environment, whereas the position of the other components is hardly affected. The results indicate that the environment of the reduced flavin in the *Desulfovibrio* flavodoxins resembles that of free reduced flavin more than in the other two flavodoxins examined. Therefore, also on the basis of the time-resolved fluorescence characteristics of reduced flavodoxin this protein can be classified into two groups: *rubrum*-like and *pasteurianum*-like. Temperature-dependent fluorescence decay studies revealed that in the temperature range used (4–37 °C) no interconversion on the fluorescence time scale between the different fluorescent states occurs.

The fluorescence anisotropy decays of the four reduced flavodoxins were measured and analyzed at different temperatures. The recovered rotational correlation times are in good agreement with those expected from the Stokes-Einstein relation for rotation of a spherical protein, indicating that the reduced protein-bound flavin is immobilized within the apoprotein matrix. The rotational correlation times of the *rubrum* class of reduced flavodoxins are somewhat longer than in *pasteurianum* flavodoxins, consistent with the larger molecular mass of the former class.

The dynamic properties of reduced flavins bound in flavodoxins as obtained from this study indicate that a specific fixed orientation of the flavin may be required for efficient electron transfer from flavodoxins to other redox proteins.

The motional behaviour of reduced flavins within the protein matrix is somewhat different from flavin bound in oxidized flavodoxins, where part of the protein population is characterized by a flavin which has a certain degree of motional freedom within the protein matrix.

The authors wish to thank Dr Ph. Bastiaens for critically reading the manuscript. Furthermore, the Netherlands Organisation for Scientific Research (N. W. O.) is thanked for partial financial support.

REFERENCES

1. Knight, E. Jr & Hardy, R. W. F. (1966) *J. Biol. Chem. 241*, 2752–2756.
2. Mayhew, S. G. (1971) *Biochim. Biophys. Acta 235*, 289–302.
3. Benemann, J. R., Yoch, D. C., Valentine, R. C. & Arnon, D. I. (1969) *Proc. Natl Acad. Sci. USA 64*, 1079–1086.
4. Vetter, H. Jr & Knappe, J. (1971) *Hoppe-Seyler's Z. Physiol. Chem. 352*, 433–446.
5. Hatchikian, E. C., LeGall, J., Bruschi, M. & Dubourdieu, M. (1972) *Biochim. Biophys. Acta 258*, 701–708.
6. van Lin, B. & Bothe, H. (1972) *Arch. Mikrobiol. 82*, 155–172.
7. Irie, K., Kobayashi, K., Kobayashi, M. & Ishimoto, M. (1973) *J. Biochem. (Tokyo) 73*, 353–366.
8. Mayhew, S. G. & Ludwig, M. L. (1975) in *The enzymes*, vol. XII (Boyer, P. D., ed.) pp. 57–118, Academic Press, New York.
9. D'Anna, J. A. Jr & Tollin, G. (1972) *Biochemistry 11*, 1073–1080.
10. Watenpaugh, K. D., Sieker, L. C. & Jensen, L. H. (1973) *Proc. Natl Acad. Sci. USA 70*, 3857–3860.
11. Burnett, R. M., Darling, G. D., Kendall, D. S., LeQuesne, M. E., Mayhew, S. G., Smith, W. W. & Ludwig, M. L. (1974) *J. Biol. Chem. 249*, 4383–4392.
12. Smith, W. W., Pattridge, K. A., Ludwig, M. L., Petsko, G. A., Tsernoglou, D., Tanaka, M. & Yasunobu, K. T. (1983) *J. Mol. Biol. 165*, 737–755.
13. van Mierlo, C. P. M., Lijnzaad, Ph., Vervoort, J., Müller, F., Berendsen, H. J. C. & de Vlieg, J. (1990) *Eur. J. Biochem. 194*, 185–198.
14. Ludwig, M. L., Pattridge, K. A., Smith, W. W., Jensen, L. H. & Watenpaugh, K. D. (1982) in *Flavins and flavoproteins* (Massey, V. & Williams, C. H., eds), pp. 19–28, Elsevier/North-Holland, Amsterdam.
15. Smith, W. W., Burnett, R. M., Darling, G. D. & Ludwig, M. L. (1977) *J. Mol. Biol. 117*, 195–225.
16. Watt, W., Tulinsky, A., Swenson, R. P. & Watenpaugh, K. D. (1991) *J. Mol. Biol. 218*, 195–208.
17. van Mierlo, C. P. M., van der Sanden, B. P. J., van Woensel, P., Müller, F. & Vervoort, J. (1990) *Eur. J. Biochem. 194*, 199–216.
18. Vervoort, J., van Berkel, W. J. H., Mayhew, S. G., Müller, F., Bacher, A., Nielsen, P. & LeGall, J. (1986) *Eur. J. Biochem. 161*, 749–756.
19. Leenders, H. R. M., Vervoort, J., van Hoek, A. & Visser, A. J. W. G. (1990) *Eur. Biophys. J. 18*, 43–55.
20. Visser, A. J. W. G., Vervoort, J., O'Kane, D. J., Lee, J. & Carreira, L. A. (1983) *Eur. J. Biochem. 131*, 639–645.
21. Karplus, M. & McCammon, J. A. (1983) *Annu. Rev. Biochem. 53*, 263–300.
22. Kraut, J. (1988) *Science 242*, 534–560.
23. Farnum, M. F., Magde, D., Howell, E. E., Hirai, J. T., Warren, M. S., Grimsley, J. K. & Kraut, J. (1991) *Biochemistry 30*, 11567–11579.
24. Rigler, R. & Ehrenberg, M. (1973) *Q. Rev. Biophys. 6*, 139–199.
25. Rigler, R. & Ehrenberg, M. (1976) *Q. Rev. Biophys. 9*, 1–19.
26. Cundall, R. B. & Dale, R. E. (eds) (1983) *NATO ASI Ser. Ser. A Life Sci. 69*.
27. Lakowicz, J. R. (1983) *Principles of fluorescence spectroscopy*, Plenum Press, New York.
28. Beechem, J. M. & Brand, L. (1985) *Annu. Rev. Biochem. 54*, 43–71.
29. Ghisla, S., Massey, V., Lhoste, J.-M. & Mayhew, S. G. (1974) *Biochemistry 13*, 589–597.
30. Visser, A. J. W. G., Ghisla, S., Massey, V., Müller, F. & Veeger, C. (1979) *Eur. J. Biochem. 101*, 13–21.
31. Visser, A. J. W. G., Ghisla, S. & Lee, J. (1991) in *Flavins and flavoproteins*, (Curti, B., Ronchi, S. & Zanetti, G., eds) pp. 49–54, Walter de Gruyter, Berlin.
32. Lee, J., Matheson, I. B. C., Müller, F., O'Kane, D. J., Vervoort, J. & Visser, A. J. W. G. (1991) in *Chemistry and biochemistry of flavoenzymes*, vol. II (Müller, F., ed.) pp. 109–151, CRC Press, Boca Raton FL.
33. LeGall, J. & Hatchikian, E. C. (1967) *C. R. Acad. Sci. Paris 264*, 2580–2583.
34. Mayhew, S. G. & Massey, V. (1969) *J. Biol. Chem. 244*, 794–802.
35. van Hoek, A. & Visser, A. J. W. G. (1992) *Proc. S. P. I. E. Int. Soc. Opt. Eng. 1640*, 325–329.
36. van Hoek, A., Vervoort, J. & Visser, A. J. W. G. (1983) *J. Biochem. Biophys. Methods 7*, 243–254.
37. van Hoek, A. & Visser, A. J. W. G. (1985) *Anal. Instrum. 14*, 359–372.
38. Visser, A. J. W. G., Ykema, T., van Hoek, A., O'Kane, D. J. & Lee, J. (1985) *Biochemistry 24*, 1489–1496.
39. van Hoek, A., Vos, K. & Visser, A. J. W. G. (1987) *I. E. E. E. J. Quantum Electron. QE-23*, 1812–1820.
40. Vos, K., van Hoek, A. & Visser, A. J. W. G. (1987) *Eur. J. Biochem. 165*, 55–63.
41. Livesey, A. K., Licinio, P. & Delaye, M. (1986) *J. Chem. Phys. 84*, 5102–5107.
42. Livesey, A. K. & Brochon, J. C. (1987) *Biophys. J. 52*, 693–706.
43. Jaynes, E. T. (1983) *Papers on probability, statistics and statistical physics*, Reidel, Dordrecht.
44. Mérola, F., Rigler, R., Holmgren, A. & Brochon, J. C. (1989) *Biochemistry 28*, 3383–3398.
45. Tauscher, L., Ghisla, S. & Hemmerich, P. (1973) *Helv. Chim. Acta 56*, 630–644.
46. Bastiaens, P. I. H., van Hoek, A., Wolkers, W. F., Brochon, J. C. & Visser, A. J. W. G. (1992) *Biochemistry 31*, 7050–7060.
47. Strickler, S. J., & Berg, R. (1962) *J. Chem. Phys. 37*, 814–822.
48. Kulinski, T., Visser, A. J. W. G., O'Kane, D. J. & Lee, J. (1987) *Biochemistry 26*, 540–549.
49. Leenders, R., Bastiaens, Ph., Lunsche, R., van Hoek, A. & Visser, A. J. W. G. (1990) *Chem. Phys. Lett. 165*, 315–322.
50. Visser, A. J. W. G., Penners, N. H. G. & Müller, F. (1983) in *Mobility and recognition in cell biology* (Sund, H. & Veeger, C., eds) pp. 137–152, Walter de Gruyter, Berlin.
51. Jablonski, A. (1965) *Acta Phys. Polon. 28*, 717–725.
52. Hansen, L. K., Christoph, G. W., Hofrichter, J. & Ludwig, M. L. (1991) in *Flavins and flavoproteins* (Curti, B., Ronchi, S. & Zanetti, G., eds) pp. 405–408, Walter de Gruyter, Berlin.
53. Pueyo, J. J., Walker, M. C., Tollin, G. & Gómez-Moreno, C. (1991) in *Flavins and flavoproteins* (Curti, B., Ronchi, S. & Zanetti, G., eds) pp. 483–486, Walter de Gruyter, Berlin.